(e.g., Zn^{2+}, Cd^{2+}) is smaller in the solvent than in water. Moreover, many reversible couples are available in these solvents as additives for stabilizing the semiconductor. For example, in this study photooxidation of compounds such as 10-MP at potentials negative of the reversible redox potential at n-GaP was observed. These photoanodic currents were stable and reproducible, showing that the n-GaP was stabilized; only two other studies of photoprocesses at n-GaP in aqueous solution showed stable behavior.[31,32] Furthermore, the larger oxidation limits of the solvent allow more positive redox couples to be employed in photoelectrochemical cells, which allow greater output voltages and potentially higher efficiencies. However, as described above, surface states can also play the role of recombination centers for the redox processes of solution species. When these are important, the maximum potential available for a cell involving a solution containing a couple with a potential E_{redox}, an electrode reversible to the couple, and an n-type semiconductor will be decreased from $E_{redox} - V_{fb}$ to $E_{redox} - E_t$. When recombination via surface states is important, chemical etching of the semiconductor, which can lead to a change in the density of such states, may be useful in obtaining better efficiencies.

Acknowledgment. We wish to thank Dr. Steven N. Frank for his continuous interest in this work. The support of this research by the National Science Foundation and the Robert A. Welch Foundation is gratefully acknowledged.

Reference and Notes

(1) (a) H. Gerischer in "Physical Chemistry: An Advanced Treatise", Vol. 9A, H. Eyring, D. Henerson, and W. Jost, Ed., Academic Press, New. York, N.Y., 1970; (b) H. Gerischer, *Adv. Electrochem. Electrochem. Eng.*, 1, 139 (1961).
(2) R. A. L. Vanden Berghe, F. Cardon, and W. P. Gomes, *Surf. Sci.*, **39**, 368 (1973).
(3) H. Kiess, *J. Phys. Chem. Solids*, **31**, 2379 (1970).
(4) H. Gerischer, *Surf. Sci.*, **18**, 97 (1969).
(5) H. Kokado, T. Nakayama, and E. Inoue, *J. Phys. Chem. Solids*, **35**, 1169 (1974).
(6) (a) R. A. L. Vanden Berghe, F. Cardon, and W. P. Gomes, *Ber. Bunsenges. Phys. Chem.*, **77**, 290 (1973); (b) *ibid.*, **78**, 331 (1974).
(7) V. A. Tyagai and G. Y. Kolbasov, *Surf. Sci.*, **28**, 423 (1971).
(8) K. H. Beckmann and R. Memming, *J. Electrochem. Soc.*, **116**, 368 (1969).
(9) B. Pettinger, H-R Schoppel, and H. Gerischer, *Ber. Bunsenges. Phys. Chem.*, **80**, 849 (1976).
(10) R. N. Noufl, P. A. Kohl, S. N. Frank, and A. J. Bard, *J. Electrochem. Soc.*, in press.
(11) S. N. Frank and A. J. Bard, *J. Am. Chem. Soc.*, **97**, 7427 (1975).
(12) D. Laser and A. J. Bard, *J. Phys. Chem.*, **80**, 459 (1976).
(13) (a) R. Landsberg, P. Janietz, and R. Dehmlow, *Z. Phys. Chem. (Leipzig)*, **257**, 657 (1976); (b) *J. Electroanal. Chem.*, **65**, 115 (1975); (c) *Z. Chem.*, **15**, 38, 106 (1975); (d) *ibid.*, **14**, 363 (1974).
(14) W. P. Gomes, T. Freund, and S. R. Morrison, *J. Electrochem. Soc.*, **115**, 818 (1968).
(15) N. E. Tokel-Takvoryan, R. E. Hemingway, and A. J. Bard, *J. Am. Chem. Soc.*, **95**, 6582 (1973).
(16) S. N. Frank, A. J. Bard, and A. Ledwith, *J. Electrochem. Soc.*, **122**, 898 (1975).
(17) V. A. Myamlin and Y. V. Pleskov, "Electrochemistry of Semiconductors", Plenum Press, New York, N.Y., 1967.
(18) (a) E. C. Dutoit, R. L. Van Meirhaeghe, F. Cardon, and W. P. Gomes, *Ber. Bunsenges, Phys. Chem.*, **79**, 1206 (1976); (b) W. H. Laflere, R. L. Van Meirhaeghe, T. Cardon, and W. P. Gomes, *Surf. Sci.*, **59**, 401 (1976).
(19) D. Laser and A. J. Bard, *J. Electrochem. Soc.*, **123**, 1837 (1976).
(20) (a) W. P. Gomes and F. Cardon, *Ber. Bunsenges. Phys. Chem.*, **74**, 432 (1970); (b) E. C. Dutoit, R. L. Van Meirhaege, F. Cardon, and W. P. Gomes, *ibid.*, **79**, 1206 (1976).
(21) B. Pettinger, H. R. Schoppel, T. Yokoyama, and H. Gerischer, *Ber. Bunsenges. Phys. Chem.*, **78**, 1024 (1974).
(22) D. Elliot, D. L. Zellmer, and H. A. Laitinen, *J. Electrochem. Soc.*, 117, 1343 (1970).
(23) L. S. R. Yeh and A. J. Bard, *Chem. Phys. Lett.*, **44**, 335 (1976).
(24) E. W. Grabner, *Electrochim. Acta*, **20**, 7 (1975).
(25) (a) A. B. Ellis, S. W. Kaiser, and M. S. Wrighton, *J. Am. Chem. Soc.*, **98**, 6418 (1976); (b) *ibid.*, **98**, 1635 (1976); (c) *ibid.*, **98**, 6855 (1976).
(26) B. Miller and A. Heller, *Nature (London)*, **262**, 680 (1976).
(27) G. Hodes, J. Manassen, and D. Cahen, *Nature (London)*, **261**, 403 (1976).
(28) S. N. Frank and A. J. Bard, *J. Am. Chem. Soc.*, **99**, 4667 (1977).
(29) T. Inoue, T. Watanabe, A. Fujushima, K. Honda, and K. Kohayakawa, *J. Electrochem. Soc.*, **124**, 719 (1977).
(30) A. J. Bard and M. S. Wrighton, *J. Electrochem. Soc.*, in press.
(31) Y. Nakato, K. Abe, and H. Tsubomura, *Ber. Bunsenges. Phys. Chem.*, **80**, 1002 (1976).
(32) A. B. Ellis, J. M. Bolts, S. W. Kaiser, and M. S. Wrighton, *J. Am. Chem. Soc.*, **99**, 2848 (1977).

Stereochemical Nonrigidity in Solid Zirconium and Hafnium Tetrakistetrahydroborates. Evidence for Two Dynamic Intramolecular Rearrangement Processes in Covalent Tridentate Tetrahydroborates

I-Ssuer Chuang, Tobin J. Marks,* [1] William J. Kennelly, and John R. Kolb

Contribution from the Department of Chemistry and the Materials Research Center, Northwestern University, Evanston, Illinois 60201. *Received March 21, 1977*

Abstract: Proton nuclear magnetic resonance studies of stereochemical dynamics in $Zr(BH_4)_4$ and $Hf(BH_4)_4$ have been carried out in the solid state. Variable temperature investigations were conducted in both continuous wave and pulsed modes. Two intramolecular motional processes were identified for each complex and the nature of these processes was interpreted on the basis of effective second moment calculations in both diffusive and positional jump regimes. The higher temperature process is assigned to rapid intramolecular bridge-terminal hydrogen exchange, $E_a(Zr) = 5.2 \pm 0.3$ ($\Delta G^{\ddagger} = 8.1$ at 214 K) l; $E_a(Hf) = 8.4 \pm 0.3$ ($\Delta G^{\ddagger} = 7.3$ at 200 K) kcal/mol. The lower temperature motion is suggested to involve rapid threefold rotation about the ligand M-B-H (terminal) axis with $E_a(Zr) = 5.4 \pm 0.2$ ($\Delta G^{\ddagger} = 4.3$ at 124 K) l; $E_a(Hf) = 4.6 \pm 0.2$ ($\Delta G^{\ddagger} = 4.4$ at 133 K) kcal/mol.

Although nuclear magnetic resonance spectroscopy has been employed to study motional processes in the solid state for a number of years,[2] two relatively recent developments promise to markedly increase activity in this area. The first is the elegant refinement of multiple pulse techniques for acquiring high-resolution information for magnetically dilute nuclei.[3] The second is the discovery that dynamic phenomena more elaborate than simple bond rotation (e.g., of methyl groups), molecular reorientation, or molecular diffusion can be observed and analyzed in the solid state. Among these more

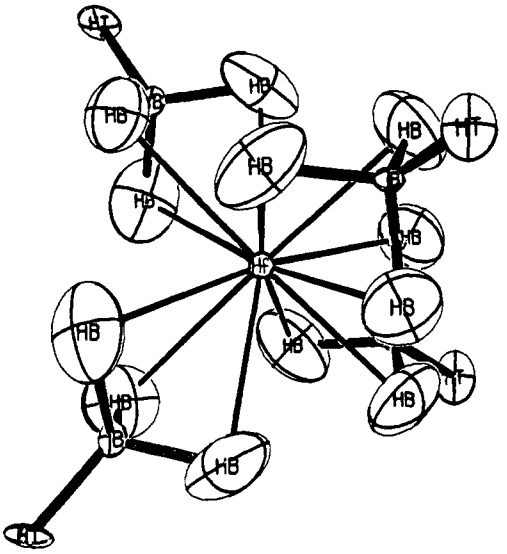

Figure 1. The molecular structure of $Hf(BH_4)_4$ as determined by neutron diffraction (ref 13c).

elaborate processes are those in which there is a rapid, degenerate, intramolecular making and breaking of chemical bonds[4] (fluxional processes[5]). The value of solid state studies becomes apparent when one considers the large number of cases where low sample solubility or the great rapidity of site exchange prevents dynamic NMR studies in solution. The solid state studies also eliminate the ambiguity as to whether the solution molecular structure of the sample is the same as that in the crystal. Furthermore, the nature of the dipolar Hamiltonian is such that positional interchange between nuclei which would be magnetically equivalent in solution (e.g., the spinning of the η^5-C_5H_5 rings in ferrocene[6]) does not escape detection in broad-line studies. Lastly, NMR investigations in the solid offer the opportunity to study stereochemical dynamics in the presence of a stringent, but relatively well-defined and ordered perturbation: the lattice, and to compare these results with solution phenomena.

Generally covalent metal tetrahydroborate complexes,[7] with few exceptions,[8] exhibit exceedingly rapid intramolecular interchange of bridge (H_b) and terminal (H_t) hydrogen atoms

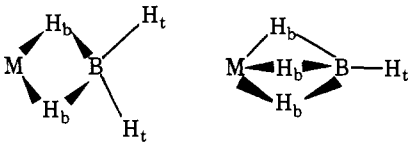

which is beyond the NMR time scale at room temperature, and in most cases, at all accessible temperatures in solution. In an effort to detect and to obtain information on the activation energetics of these very rapid processes, we have taken three approaches. The first was to expand the time resolution of the ^1H NMR experiment[7,9] by greatly increasing the difference in resonance energies between bridge and terminal sites. This was successful in the case of $(\eta^5$-$C_5H_5)_3UBH_4$[10] (which has a tridentate ground-state geometry) and the free energy of activation at spectral coalescence (133 ± 20 K) was found to be 5.0 ± 0.6 kcal/mol.[10] The second tack has been to investigate molecules where electronic considerations or vibrational spectroscopic data suggest that the metal–ligand bonding might be more rigid, i.e., that the ground-state configuration might lie in a deeper potential well so that bridge–terminal hydride exchange would be slower. For the bidentate complexes $(\eta^5$-$C_5H_5)_2VBH_4$[11] and $[(C_6H_5)_3P]_2N^+Mo(CO)_4$-$BH_4^-$,[12] this was found to be the case, and free energies of activation respectively of 7.6 ± 0.3 (186 ± 7 K) and 10.1 ± 0.2 kcal/mol (231 ± 4 K) were found.

A third approach to studying rapid tetrahydroborate bridge–terminal hydrogen interchange is by NMR in the solid state, a technique which offers the unique features cited above. The purpose of this article is to discuss our results on the tridentate complexes $Zr(BH_4)_4$ and $Hf(BH_4)_4$. Here, the molecular structures are known with considerable precision[13] and the rate of bridge–terminal hydrogen interchange is too rapid to measure in solution, even with decoupling of quadrupolar ^{11}B.[14] Besides providing the first quantitative information on the rate of the fluxional process in the solid, our results also assign the presence of another dynamic intramolecular process, heretofore unknown.

Experimental Section

The extremely air-sensitive complexes $Zr(BH_4)_4$ and $Hf(BH_4)_4$ were prepared by the procedure of James and Smith,[15] and were handled under prepurified nitrogen or in vacuo at all times. Samples for NMR studies were sublimed twice on a vacuum line and were then sealed, under vacuum, in 11-mm outside diameter quartz tubes. As a check for purity, laser Raman spectra were recorded of the sealed samples and were found to be identical with published spectra.[16]

Nuclear Magnetic Resonance Studies. Continuous wave ^1H measurements were performed at 16 MHz on a wide-line spectrometer employing a Varian V-3703 electromagnet with a Fieldial Mark I power supply, and a Hill-Hwang[17] marginal oscillator. Sample temperature control was maintained with an Oxford Instruments DTC-2 precision temperature controller which applied the required heating to the sample chamber of the liquid nitrogen cooled variable temperature Dewar. A copper–constantan thermocouple was attached with Teflon tape directly to the sample tube. Ample time was allowed for equilibration at each new temperature; at least three derivative spectra were recorded at each temperature. In addition, spectra at a given temperature were recorded in the process of both going to and coming from lower temperatures; in all cases the results were identical. Pains were also taken to avoid signal distortion due to rf saturation or overmodulation. Experimental second moment calculations were performed using a local computer program similar in logic to that of Smith;[18] corrections for finite modulation amplitudes were made in the experimental data.[19] For theoretical second moments, internuclear distances were calculated from the diffraction-determined coordinates[13] using the program NUDAPA.[20] The exact intermolecular contribution to the second moment was calculated to cutoff distances of 6.0 and 9.0 Å. Beyond this, the value was approximated.[21]

Pulsed NMR measurements were made at 16 MHz on a spectrometer constructed with a Varian V-3603 electromagnet, an Arenberg PG-650C rf transmitter, and an Arenberg WA-600D wide-band power amplifier. Spin–lattice relaxation times were measured by the 180°–τ–90°[22] technique using a Princeton Applied Research CW-1 boxcar integrator to integrate the y axis magnetization. Sample temperature regulation was the same as for the CW spectrometer.

Results

Structural Considerations. The molecular structure of $Zr(BH_4)_4$ has been determined by single crystal x-ray diffraction at 113 K[13a] and by gas-phase electron diffraction.[13b] The structure of $Hf(BH_4)_4$ has been studied at 79 and 24 K by single crystal neutron diffraction.[13c] The results for these isostructural molecules are in substantial agreement, with four tridentate tetrahydroborate ligands coordinated to the metal in a tetrahedral array. The neutron diffraction results are displayed in Figure 1.

Continuous Wave NMR Results. The ^1H NMR line width of polycrystalline $Hf(BH_4)_4$ as a function of temperature is shown in Figure 2A. The second moments of the line shapes,[2] as defined in

$$S = \frac{\int_{-\infty}^{\infty} (H - H_0)^2 f(H) \mathrm{d}H}{\int_{-\infty}^{\infty} f(H) \mathrm{d}H} \qquad (1)$$

Table I. Line Width and Second Moment Data for $Zr(BH_4)_4$ and $Hf(BH_4)_4$

Compd and temp	Exptl line width, G	Exptl second moment, G^2	Process	Calcd second moment diffusive, G^2	Calcd second moment jump, G^2
$Zr(BH_4)_4$, <120 K	17.0 ± 1.0	44.8 ± 0.4	Rigid lattice	53.5	53.5
155 K ≤ T ≤ 180 K	8.0 ± 0.1	12.5-14.7	BH_4^- rotation[a]	18.3	17.0
240 K ≤ T ≤ 290 K	5.5 ± 0.1	5.2-5.3	Fluxional[b]	4.6	4.4
			Overall molecular reorientation	1.3	1.0
$Hf(BH_4)_4$, <120 K	19.1 ± 1.0	48.7 ± 1.7	Rigid lattice	54.8	54.8
155 K ≤ T ≤ 180 K	8.0 ± 0.1	13.7-15.6	BH_4^- rotation[a]	19.2	17.3
240 K ≤ T ≤ 290 K	6.1 ± 0.1	4.9-5.3	Fluxional[b]	5.1	4.9
			Overall molecular reorientation	1.3	1.0

[a] Process depicted in eq 10. [b] Process depicted in eq 11.

are plotted in Figure 2B vs. temperature. The results for $Zr(BH_4)_4$ are nearly identical, and data for both molecules are summarized in Table I. the second moment can be related to the rigid lattice molecular structure by the Van Vleck formula, suitably modified for a polycrystalline sample:[2]

$$S = \frac{6}{5} I_i(I_i + 1)g^2{}_i\beta^2 N_i^{-1} \sum_{i>j} r_{ij}^{-6} + \frac{4}{15}\beta^2 N_i^{-1} \sum_{i,k} I_k(I_k + 1)g^2{}_k r_{ik}^{-6} \quad (2)$$

Here i and j refer to protons, k to nonresonant nuclei (^{10}B, ^{11}B, Zr, Hf), and the other terms have their usual meaning. Besides the internuclear dipolar interaction described by eq 2 three other interactions could conceivably complicate the relationship between the observed and calculated second moments. The most significant of these terms arises in the boron-proton component of the second moment if the ^{10}B (18.8% abundant) and ^{11}B (81.2% abundant) nuclear quadrupolar interactions are larger than the respective Zeeman interactions.[23] This leads to quantization of the boron spin vector in a direction other than that of the static field H_0 (i.e., toward the z axis of the field gradient tensor) and to anomalously large observed second moments. For this perturbation to be significant, the α factor in

$$\alpha = \left|\frac{4I_k(2I_k - 1)g_k\beta H_0}{e^2qQ}\right| \quad (3)$$

must be less than ca. 10-20. Here, the denominator is the nuclear quadrupole coupling constant (the field gradient about boron is axially symmetric). For zirconium and hafnium which have isotopes with nuclear quadrupole moments, the cubic symmetry assures that $e^2qQ = 0$. For the $M(BH_4)_4$ compounds the nuclear quadrupole coupling constants were found[14a] to be 1.7 ± 0.3 (^{11}B) and 3.5 ± 0.6 MHz (^{10}B), which yield α values of 31.4-44.0 (^{11}B) and 25.1-35.6 (^{10}B). Thus, the "indirect" dipolar interaction should not introduce appreciable error in theoretical second moments calculated with the Van Vleck equation. Another possible source of error arises in cases where internuclear scalar coupling is large enough to contribute to the second moment via:[23b]

$$S = \frac{I_i(I_i + 1)}{3} J^2 \quad (4)$$

In solution,[14a] $J_{^{11}B\text{-}H}$ = 90.0 (Zr), 88.6 (Hf), and $J_{^{10}B\text{-}H}$ = 30.0 (Zr), 29.6 (Hf) Hz, so that any effects arising from these terms are calculated to be on the order of $0.001G^2$, which is undetectable. Finally, any proton chemical shift anisotropy would lead to errors; fortunately proton chemical shift anisotropies are expected to be quite small.[24] Thus, eq 2 is applicable to the present problem.

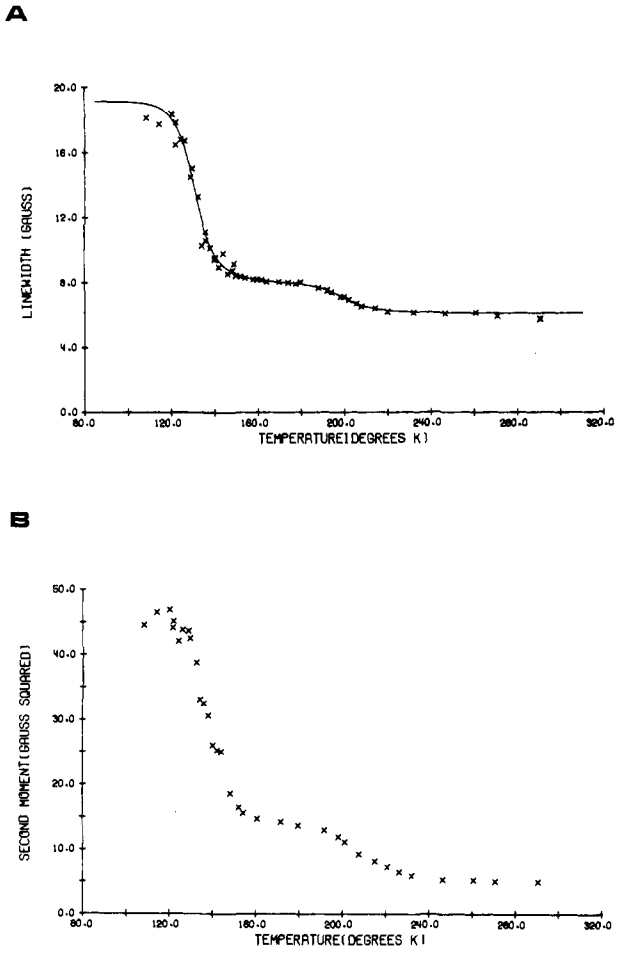

Figure 2. A. Plot of the experimental ^1H NMR line width vs. temperature for a polycrystalline sample of $Hf(BH_4)_4$. The points represent an average of three to five measurements. The solid line is a least-squares fit to eq 7. B. Plot of experimental second moments vs. temperature for a polycrystalline sample of $Hf(BH_4)_4$. The points represent an average of three to five measurements.

Table I presents experimental second moment data for $Zr(BH_4)_4$ and $Hf(BH_4)_4$ along with estimated standard deviations for these measurements. Also given are calculated rigid lattice second moments based upon the structural data. The agreement between experimental and calculated rigid lattice second moments was slightly better when B-H distances from the tridentate BH_4^- group in the neutron diffraction study of $U(BH_4)_4$[25a] were used. Since the second moments are proportional to $1/r^6$, they are extremely sensitive to small structural inaccuracies,[25b] and the uranium structure determination

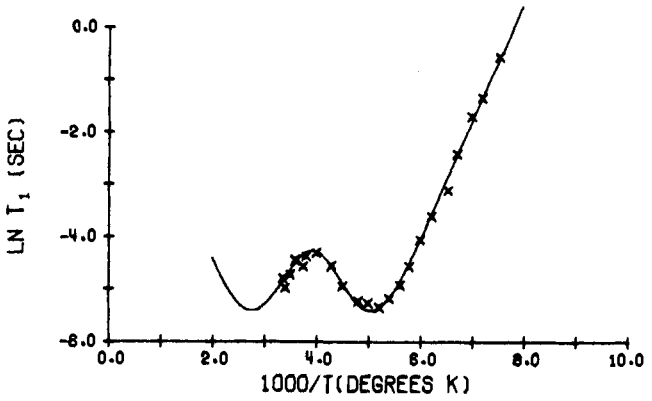

Figure 3. Plot of the natural logarithm of the proton spin-lattice relaxation time vs. inverse temperature for a polycrystalline sample of $Hf(BH_4)_4$. The solid line corresponds to a least-squares fit to eq 6 with $C = C'$ as described in the text.

was of somewhat better quality. As can be seen, the agreement between experimental and calculated rigid lattice second moments is generally good. It is unlikely that appreciable molecular motion is occurring at 100 K, and any discrepencies between experimental and calculated S values are easily attributed to saturation effects since in this temperature region the proton spin-lattice relaxation times are very long (vide infra). As the temperature is raised, line narrowing in $Hf(BH_4)_4$ occurs (Figure 2) and continues until ca. 170 K. The line width then remains constant until ca. 180 K, when a second narrowing process is observed. Above ca. 220 K, the line width remains constant until the compound melts at 302 K. That this line narrowing is due to the successive onset of two rapid motional processes rather than phase transitions is supported by T_1 measurements (vide infra). Furthermore, no evidence for phase transitions has been noted in the structural studies. The line narrowing is completely reversible on lowering the temperature. The variable temperature behavior of $Zr(BH_4)_4$ is similar (Table I) but not identical.

Pulsed NMR Results. Figure 3 presents proton spin-lattice relaxation time (T_1) data for $Hf(BH_4)_4$ as a function of temperature. The classical expression for spin-lattice relaxation by motional modulation of nuclear dipolar interactions (by a single motional process) is given by[2]

$$\frac{1}{T_1} = C\left(\frac{\tau_c}{1+\omega^2\tau_c^2} + \frac{4\tau_c}{1+4\omega^2\tau_c^2}\right) \quad (5)$$

where C depends on the particular interacting nuclei and their spatial relationship, $\omega/2\pi$ is the Larmor frequency, and τ_c is the correlation time for the motion. Though this equation was originally derived for spin pairs, it is generally found to be a reasonable approximation of relaxation behavior in more complicated systems. Equation 6 is applicable in cases where two motional processes occur.[26] It predicts a minimum in the plot of ln T_1 vs. $1/T$ for each process.

$$\frac{1}{T_i} = C\left(\frac{\tau_{c_1}}{1+\omega^2\tau_{c_1}^2} + \frac{4\tau_{c_1}}{1+4\omega^2\tau_{c_1}^2}\right) + C'\left(\frac{\tau_{c_2}}{1+\omega^2\tau_{c_2}^2} + \frac{4\tau_{c_2}}{1+4\omega^2\tau_{c_2}^2}\right) \quad (6)$$

The pattern observed in Figure 3 is characteristic of the presence of two correlated motional processes.[26] The low-temperature process is readily evident. The onset of a second, higher temperature process is observed, but owing to the relatively fast time scale of the measurement technique at this frequency, melting takes place before the minimum is reached. It will be shown that the two motional processes observed in the pulsed experiments are kinetically identical with those defined in the CW studies. There is no evidence of a phase transition which is characterized by an abrupt discontinuity in the ln T_1 vs. $1/T$ plot. Figure 3 also shows a least-squares fit of the relaxation time data to eq 6 assuming thermal activation (vide infra). There is no evidence in the magnetization recovery plots of appreciable nonexponential behavior. This is sometimes observed in reorienting methyl groups and is indicative of relaxational cross-correlation effects.[27a] Other causes of nonexponentiality have been identified as cross-relaxation[27b] and T_1 anisotropy.[27c]

Kinetic Data Analysis. For the presence of two motional processes it is possible to express the line width as in[28]

$$(\Delta H)^2 = C^2 + (A^2 - B^2)2/\pi\left[\tan^{-1}\frac{\alpha\tau\Delta H}{2\pi\nu_{c_1}}\right] + (B^2 - C^2)2/\pi\left[\tan^{-1}\frac{\alpha\gamma\Delta H}{2\pi\nu_{c_2}}\right] \quad (7)$$

Here A, B, and C are the rigid lattice line width, the line width when the first motional process is rapid ($\nu_{c_1} \gg \alpha\gamma\Delta H$ at ca. 170–180 K in the present case), and the high temperature line width ($\nu_{c_1}, \nu_{c_2} \gg \alpha\gamma\Delta H$ at $T > 220$ K), respectively. The ν_c's are the correlation frequencies ($\nu_c = (2\pi\tau_c)^{-1}$) for the low ($\nu_{c_1}$) and high ($\nu_{c_2}$) temperature processes, and the other terms have their usual meaning.[28] Figure 2A illustrates a least-squares fit to the line width data. The agreement is quite satisfactory. If it is assumed that the dynamic processes are thermally activated, i.e.,

$$\tau_{c_i} = \tau_{0_i} e^{E_{a_i}/RT} \quad (8)$$

is valid, then it is possible to derive activation energies for the two motional processes by solving eq 7 for the cases where $\nu_{c_2} \to 0$ (110 K $\lesssim T \lesssim$ 170 K), $\nu_{c_1} \to \infty$ ($T \gtrsim$ 180 K). Fitting plots of ln ν_{c_i} vs. $1/T$ by least squares yielded E_a values for $Hf(BH_4)_4$ of 4.6 ± 0.2 (low-temperature process) and 8.4 ± 0.3 kcal/mol (high-temperature process). The activation parameters for $Zr(BH_4)_4$ are roughly the same; data are set out in Table II. Because of inherent errors in fitting Arrhenius plots, more reliable $\Delta G^{\ddagger}$ values,[33] calculated from

$$1/\tau_{c_i} = (kT/h)e^{\Delta G^{\ddagger}/RT} \quad (9)$$

at the midpoints of the narrowing regions, are also presented. It is also possible to derive activation parameters from the pulsed NMR data. From eq 6 and 8,[2] a least-squares fit of the data for $Hf(BH_4)_4$ (Figure 3) yields an activation energy for the low-temperature motional process of 4.5 ± 0.2 kcal/mol, which is in excellent agreement with the results from the line width studies. We are reluctant to attempt to derive an accurate E_{a_2} from the scanty pulsed data in this temperature region. From the least-squares fit to eq 6 (Figure 3) it is evident that the minimum (at 16 MHz) in the ln T_1 vs. $1/T$ plot will be at ca. 360 K, which is above the melting point. Studies at significantly lower frequencies, which would increase the effective spectral time scale, suffered from loss in sensitivity and interference with the ^{19}F signal of the Teflon sample holding apparatus.[29]

Mechanistic Discussion. Though the foregoing section has established the presence and activation energetics for two dynamic motional processes in $Zr(BH_4)_4$ and $Hf(BH_4)_4$, the nature of these processes is of great interest and remains to be discussed. Three kinds of processes are conceivable: self-diffusion, overall molecular reorientation, and intramolecular rearrangement of the tetrahydroborate ligands as in the bridge-terminal hydrogen interchange observed in solution. As will be seen, it is possible to numerically estimate the effects of each of these processes on the observed line widths and second moments.

Self-diffusion has been observed in several molecular systems, e.g., cyclohexane[2a] and one phase of $Si(CH_3)_4$.[30a] The

Table II. Activation Parameters for Motional Processes in $Zr(BH_4)_4$ and $Hf(BH_4)_4$[a]

Compd	E_a,[b] kcal/mol	$\alpha\tau_0$,[b] s × 10^{-14}	$\Delta G^{\ddagger}$, kcal/mol[c]	E_a,[d] kcal/mol	τ_0,[d] s × 10^{-14}
$Zr(BH_4)_4$					
Low-temperature process	5.4 ± 0.2	0.09	4.3 (124 K)		
High-temperature process	5.2 ± 0.3	3820	7.3 (200 K)		
$Hf(BH_4)_4$					
Low-temperature process	4.6 ± 0.2	3.56	4.6 (133 K)	4.5 ± 0.2	6.07
High-temperature process	8.4 ± 0.3	0.304	8.1 (214 K)		

[a] Standard deviations are derived from least-squares fits to the appropriate equations. [b] Continuous wave data using eq 7 and 8. [c] From eq 9, taken at the midpoint of the narrowing process. [d] Pulsed data using eq 6 and 8.

rapid isotropic molecular motion averages all dipolar interactions and leads to spectral line widths which approach those observed in fluid solution. This type of behavior is not observed for $Zr(BH_4)_4$ and $Hf(BH_4)_4$ and it is safe to conclude that self-diffusion is not an important line-narrowing process. Rapid molecular reorientation averages intra- and intermolecular dipolar interactions in a predictable manner. Rapid isotropic overall reorientation will average the intramolecular component of the calculated rigid lattice second moment (ca. 49 G^2 out of ca. 55 G^2) to zero.[2] Likewise, the cubic molecular and lattice symmetry in the present case ensures that there is an equal probability for reorientation about symmetry-related molecular axes, and again the intramolecular part of the second moment averages to zero.[30b] The reduction of the intermolecular part of the rigid lattice second moment can be calculated for the two extreme descriptions of molecular reorientation. For the case of a classical diffusive process in which all atoms can be considered to be moving with constant angular velocity on the surfaces of spheres centered at the metal ion, the center-to-center method of second moment calculation is rigorously applicable and has been used with considerable success.[31] By this procedure we calculate a total second moment of 1.3 G^2, which is far below either of the experimental leveling-off values observed in the present case. An alternative description of isotropic molecular reorientation is the "jump model" in which each of the hydrogen atoms in the molecule jumps between symmetry-equivalent positions. The problem becomes one of averaging terms of the type $(3\cos^2\theta - 1)/r^3_{ij}$ between intermolecular pairs of nuclei i and j over all possible relative positions, and also averaging over all orientations for a powder sample. This can be done by an expansion utilizing the addition theorem of associated Legendre polynomials (see Appendix for details). By this procedure we calculate a theoretical second moment of 1.0 G^2. Again the theoretical value is far smaller than either of the observed, narrowed second moments, and it is clear that overall molecular reorientation does not make a significant contribution to the spectral line narrowing.

The above results indicate that the motional processes observed by NMR in $Zr(BH_4)_4$ and $Hf(BH_4)_4$ must be intramolecular in nature. Since *two* regions of spectral narrowing are observed, any accurate description of the molecular dynamics must incorporate two intramolecular processes. It is reasonable to postulate and then to test by calculation that one of the two processes is the bridge-terminal hydrogen interchange process. For the second process we shall examine BH_4^- rotation about the M–B–H_t axis. This rearrangement can be most easily viewed by Newman projections (eq 10).

The plausibility of this rotational mechanism is supported by the fact that both the electron and neutron diffraction studies revealed large thermal amplitudes along this rotational coordinate,[13] suggestive of a shallow potential well. Furthermore, this process is analogous to ring rotation in η^5-C_5H_5,[6] η^6-C_6H_6,[28] and η^8-C_8H_8[32] organometallics.

We first calculate the effect which rotation of the ligands about the M–B–H_t axes would have on the second moment of

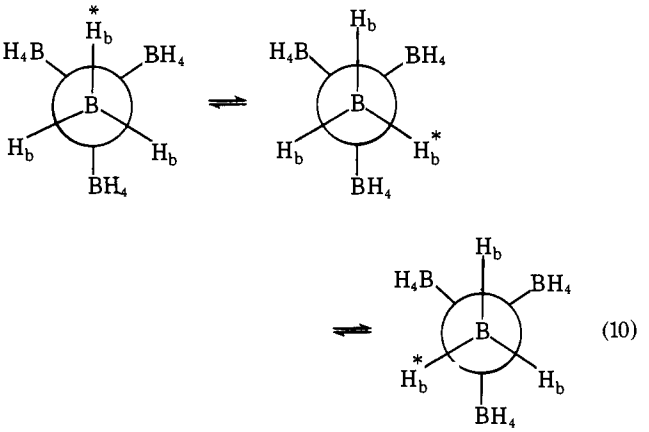

$Hf(BH_4)_4$. Two extreme descriptions of the rearrangement are possible: a diffusive (constant angular velocity) or a three-position jump process. For the diffusive reorientation, the intra-BH_4^- contribution to the second moment will be reduced by a factor of $\frac{1}{4}(3\cos^2\alpha_{ij} - 1)^2$,[2] where α_{ij} is the angle between the internuclear vector r_{ij} and the rotation axis. The intramolecular inter-BH_4^- and intermolecular inter-BH_4^- contributions can be calculated in this case by a center-to-center method[31] in which the three H_b nuclei of each BH_4^- group are placed at the point where their plane intersects the rotation axis. This procedure yields an estimated total effective second moment of 19.2 G^2. For the three-position jump model, which is probably a more accurate description of eq 10, it can be shown that the intra-BH_4^- portion of the second moment will again be reduced by $\frac{1}{4}(3\cos^2\alpha_{ij} - 1)^2$.[31a,30b] The intramolecular inter-BH_4^- and intermolecular inter-BH_4^- components of the second moment were rigorously calculated in this description by the Lengendre polynomial expansion averaging procedure (see Appendix). Combining these results yields a total theoretical second moment for the three-position ligand jump rotational model of 17.3 G^2. In comparison the experimental effective second moment of $Hf(BH_4)_4$ for the low-temperature process in the relatively level region of 155–180 K is in the range 15.6–13.7 G^2. These values are in reasonable agreement with the rotational jump model especially considering that there is some overlap of the two motional processes and that there may be slight inaccuracies in the experimental bond distances (vide supra) of $Hf(BH_4)_4$. The results of these calculations and those on $Zr(BH_4)_4$ are summarized in Table I.

The second, higher temperature dynamic process must necessarily be one which results in greater motional averaging of the internuclear dipolar interactions than the ligand rotation and thus produces a smaller effective second moment. It is possible to describe the bridge-terminal hydrogen interchange process (eq 11) both in terms of diffusive BH_4^- reorientation

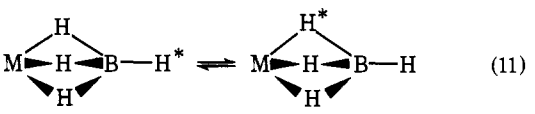

and in terms of a four-position jump model. In either case the contributions to the total second moment can be divided into intra-BH_4^-, intramolecular inter-BH_4^-, and intermolecular inter-BH_4^- parts. For both diffusive and jump models, the intra-BH_4^- component goes to zero in the regime where this tumbling motion of the tetrahydroborate ligand becomes rapid. For the diffusive process, the intramolecular inter-BH_4^- and intermolecular inter-BH_4^- contributions to the second moment can be calculated by the center-to-center method described above. This yields a total effective second moment for $Hf(BH_4)_4$ of 5.1 G^2. For the jump model, the intramolecular inter-BH_4^- second moment contribution was rigorously computed using the Lengendre polynomial expansion averaging procedure mentioned earlier (see Appendix) as was the intermolecular inter-BH_4^- component. This averaging procedure yields a total effective second moment of 4.9 G^2 for the four-position jump model. Reference to Table I and Figure 2a shows that above 240 K, the experimental second moment for $Hf(BH_4)_4$ is in the range 5.3–4.9 G^2, which is in excellent agreement with the theoretical values for both descriptions of the fluxional process in eq 11. Analogous results for $Zr(BH_4)_4$ are also presented in Table I.

Conclusions

The two motional processes observed in solid state ^1H NMR spectra of both $Zr(BH_4)_4$ and $Hf(BH_4)_4$ are assigned to dynamic intramolecular rearrangements. The process which results in the greatest line narrowing ($E_a(Zr) = 5.2 \pm 0.3$; $E_a(Hf) = 8.4 \pm 0.3$ kcal/mol) is ascribed, on the basis of second moment calculations, to rapid bridge-terminal hydrogen permutation (eq 11), a phenomenon already suggested by 90-MHz ^1H studies in solution.[7,14] Here negligible line broadening was observed down to 193 K in toluene-d_8.[14] Whether incorporation in a crystal lattice has significantly changed the barrier to rearrangement is difficult to estimate, principally owing to the paucity of solution rate data. The barriers for bridge–terminal interchange found in the present case are roughly comparable to that found for the tridentate $(C_5H_5)_3UBH_4$ ($\Delta G^{\ddagger} \approx 5.0 \pm 0.6$ kcal/mol at 133 K). For $Zr(BH_4)_4$ and $Hf(BH_4)_4$, if it is assumed that the mean preexchange proton site lifetime in solution, τ, is less than 10^{-4} s at 193 K, then from eq 9,[33] $\Delta G^{\ddagger} \lesssim 9.3$ kcal/mol. From the broad-line data and eq 9 $\Delta G^{\ddagger}(Zr)$ and $\Delta G^{\ddagger}(Hf) \approx 7.4$ kcal/mol at 193 K. From these data and similar studies on fluxional organometallics in the solid state,[4] it appears that lattice effects on activation energies are at most on the order of a few kcal/mol. Ironically, it is the lack of accurate solution rate data which prevents more detailed conclusions.

A second, lower temperature dynamic process was also identified in the $M(BH_4)_4$ solids, with $E_a(Zr) = 5.4 \pm 0.2$ and $E_a(Hf) = 4.6 \pm 0.2$ kcal/mol. This motion results in less line narrowing at fast exchange than the bridge–terminal hydrogen interchange process and is already rapid at the onset of the latter process. On the basis of effective second moment calculations this motion is postulated to involve rotation of the coordinated BH_4^- ligands about the M–B–H_t axes (eq 9). Large thermal vibrational amplitudes along this coordinate were identified in both the neutron[13c] and electron diffraction[13b] studies of these compounds, and the situation is, as stated previously, completely analogous to ($\eta^n = C_nH_n$)M molecules where libration is frequently apparent in diffraction results and where rapid motion is observed in broad-line NMR studies.[6,28,32] The molecular orbitals of a tridentate BH_4^- ligand are similar in energy and symmetry to an $\eta^n = C_nH_n$ carbocycle,[7a,35] which is in accord with a relatively low barrier to rotation.

It is also interesting to compare BH_4^- motion in the present covalent cases with motion in ionic alkali metal tetrahydroborates.[36] The latter undergo BH_4^- tumbling with barriers of 2.7–4.7 kcal/mol, depending on the alkali metal and the crystalline phase. Only one motional process is evident for a given type of ionic BH_4^- group in a given phase.

Acknowledgments. We are grateful to the National Science Foundation (CHE 74-10341 A02 and DMR 72-03019 A06) for generous support of this work. We thank Drs. N. Karnezos and W. Spurgeon for help advice and assistance, and R. W. Marks for a copy of ref 18.

Appendix

The general equation for the second moment of an NMR signal in the case of a cingle crystal with a rigid lattice is given by

$$S = 3/4g_i^4\beta^2N_i^{-1}I(I+1)\sum_{i\neq j}(1-3\cos^2\theta_{ij})^2/r_{ij}^6 \quad \text{(A1)}$$

(eq 2 is derived from this), where r_{ij} is the distance between nuclei i and j, θ_{ij} is the angle between the static field and the internuclear vector, and the other terms have their usual meaning. For $(1-3\cos^2\theta)/r_{ij)/rij}^3$ we desire to take a temporal average (denoted by $\langle\ \rangle$) to account for molecular motion (r_{ij} and θ_{ij} become time dependent) and a spatial average (denoted by [ ]) for powder samples. By the addition theorem of Lengendre polynomials,[37]

$$\left[\left\langle\frac{1-3\cos^2\theta}{r^3}\right\rangle^2\right] = 1/5\left\langle\frac{3\cos^2\delta-1}{r^3}\right\rangle^2 + 3/5\left\{\left\langle\frac{\sin 2\delta\cos\varphi}{r^3}\right\rangle^2 + \left\langle\frac{\sin 2\delta\sin\varphi}{r^3}\right\rangle^2 + \left\langle\frac{\sin^2\delta\cos 2\varphi}{r^3}\right\rangle^2 + \left\langle\frac{\sin^2\delta\sin 2\varphi}{r^3}\right\rangle^2\right\} \quad \text{(A2)}$$

can be derived for each nuclear pair i, j, where r, δ, and φ are the spherical polar coordinates of internuclear vector **r** in an arbitrary reference coordinate system. The equation

$$\left[\left\langle\frac{1-3\cos^2\theta}{r^3}\right\rangle^2\right] = 1/5\left\langle\frac{3z^2-r^2}{r^5}\right\rangle^2 + 3/5\left\{\left\langle\frac{2xz}{r^5}\right\rangle^2 + \left\langle\frac{2yz}{r^5}\right\rangle^2 + \left\langle\frac{x^2-y^2}{r^5}\right\rangle^2 + \left\langle\frac{2xy}{r^5}\right\rangle^2\right\} \quad \text{(A3)}$$

follows on changing to Cartesian coordinates, where x, y, z are the coordinates of vector **r**. This equation can be readily incorporated into a computer program[38] for calculating effective second moments under different types of motional averaging. Equation A3 is equivalent to expressions derived by Watton et al.[39] and Andrew et al.[40]

For multiposition jump[30b] descriptions of molecular motion in $M(BH_4)_4$, the procedures given below were employed. The numerical results were summarized in Table I.

(1) Rotation about M–B–H (terminal) axes. Terms on the right-hand side of eq A3 were calculated for each internuclear pair, averaging over the three possible sites that each bridge hydrogen could occupy (with equal probability). Second moments calculated for cutoff radii of 6.0 and 9.0 Å were within 0.1 G^2.

(2) Bridge–terminal hydrogen interchange. A calculation was performed as above, but with each BH_4^- hydrogen having access, with equal probability, to four sites. Computed second moments with 6.0 and 9.0 Å cutoff radii were within 0.1 G^2.

(3) Molecular reorientation (with rigid BH_4^- groups). In this case, the intramolecular internuclear distances remained constant, and each BH_4^- ligand had access to four sites, with three orientations in each site. As expected, the intramolecular component of the effective second moment was calculated to be zero. Second moments for 6.0 and 9.0 Å cutoff radii were essentially identical.

(4) Molecular reorientation combined with rotation about the M-B-H (terminal) axes, and molecular reorientation combined with bridge-terminal hydrogen interchange. In these cases, intramolecular internuclear distances must also be averaged in the calculation. For the former process (6.0 or 9.0 Å cutoff) the effect second moment was calculated to be 1.0 G^2, while for the latter process (6.0 or 9.0 Å cutoff) it was computed to be 0.9 G^2.

References and Notes

(1) (a) Fellow of the Alfred P. Sloan Foundation. (b) Camille and Henry Dreyfus Teacher-Scholar.
(2) (a) E. R. Andrew, "Nuclear Magnetic Resonance", Cambridge University Press, London, 1955, Chapter 6; (b) C. P. Slichter, "Principles of Magnetic Resonance", Harper and Row, New York, N.Y., 1963, Chapters 3 and 5; (c) A. Abragam, "The Principles of Nuclear Magnetism", Oxford University Press, London, 1961, Chapters IV, VIII, IX, and X.
(3) (a) U. Haeberlen, *Adv. Magn. Reson., Suppl.*, 1 (1976); (b) M. Mehring, *NMR*, 11, 1 (1976); (c) R. K. Hester, V. R. Cross, J. L. Ackerman, and J. S. Waugh, *J. Chem. Phys.*, **63**, 3606 (1975); (d) A. Pines, M. S. Gibby, and J. S. Waugh, *J. Chem. Phys.*, **59**, 569, (1973); (e) P. Mansfield, *Prog. Nucl. Magn. Reson. Spectrosc.*, **8**, 41 (1971).
(4) (a) A. J. Campbell, C. A. Fyfe, and E. Maslowsky, Jr., *J. Am. Chem. Soc.*, **94**, 2690 (1972); (b) A. J. Campbell, C. A. Fyfe, R. G. Goel, E. Maslowsky, Jr., and C. V. Senoff, *ibid.*, **94**, 8387 (1972); (c) A. Chierico and E. R. Mogaschi, *J. Chem. Soc., Faraday Trans. 2*, **69**, 433 (1973); (d) R. T. Paine, E. Fukushima, and S. B. W. Roeder, *Chem. Phys. Lett.*, **32**, 566 (1975); (e) A. J. Campbell, C. E. Cottrell, C. A. Fyfe, and K. R. Jeffrey, *Inorg. Chem.*, **15**, 1321, 1326 (1976).
(5) (a) F. A. Cotton in "Dynamic Nuclear Magnetic Resonance Spectroscopy", L. M. Jackman and F. A. Cotton, Ed., Academic Press, New York, N.Y., 1975, Chapter 10; (b) J. P. Jesson and E. L. Muetterties in ref 5a, Chapter 8.
(6) L. N. Mulay and A. Attalla, *J. Am. Chem. Soc.*, **85**, 702 (1963), and references cited therein.
(7) (a) T. J. Marks and J. R. Kolb, *Chem. Rev.*, 77, 263 (1977); (b) B. D. James and M. G. H. Wallbridge, *Prog. Inorg. Chem.*, 11, 99 (1970).
(8) H. D. Empsall, E. Mentzer, and B. L. Shaw, *J. Chem. Soc., Chem. Commun.*, 861 (1975).
(9) (a) H. S. Gutowsky and H. N. Cheng, *J. Chem. Phys.*, **63**, 2439 (1975); (b) S. R. Tanny, M. Pickering, and C. S. Springer, *J. Am. Chem. Soc.*, **95**, 6227 (1973).
(10) T. J. Marks and J. R. Kolb, *J. Am. Chem. Soc.*, **97**, 27 (1975).
(11) T. J. Marks and W. J. Kennelly, *J. Am. Chem. Soc.*, **97**, 1439 (1975).
(12) S. W. Kirtley, M. A. Andrews, R. Bau, G. W. Grynkewich, T. J. Marks, D. L. Tipton, and B. R. Whittlesey, *J. Am. Chem Soc.*, in press.
(13) (a) P. H. Bird and M. R. Churchill, *Chem. Commun.*, 403 (1967); (b) V. Plato and K. Hedberg, *Inorg. Chem.*, **10**, 590 (1971); (c) E. R. Bernstein, W. C. Hamilton, T. A. Keiderling, W. J. Kennelly, S. J. La Placa, S. J. Lippard, T. J. Marks, and J. J. Mayerle, unpublished neutron diffraction results at Brookhaven National Laboratory. See ref 7a for more details.
(14) (a) T. J. Marks and L. A. Shimp, *J. Am. Chem. Soc.*, **94**, 1542 (1972); (b) unpublished results.
(15) B. D. James and B. E. Smith, *Synth. React. Inorg. Met.-Org. Chem.*, **4**, 461 (1974).
(16) (a) T. J. Marks, W. J. Kennelly, J. R. Kolb, and L. A. Shimp, *Inorg. Chem.*, 11, 2540 (1972); (b) T. A. Keiderling, W. T. Wozniak, R. S. Gay, D. Jurkowitz, E. R. Bernstein, S. J. Lippard, and T. G. Spiro, *ibid.*, **14**, 576 (1975).
(17) D. A. Hill and C. Hwang, *J. Sci. Instrum.*, **43**, 581 (1966).
(18) G. W. Smith, *Gen. Mot. Corp., Res. Lab., Res. Publ.*, GMR-540 (1966).
(19) E. R. Andrew, *Phys. Rev.*, **91**, 425 (1953).
(20) We thank Professor J. A. Ibers for the use of this program.
(21) J. A. Ibers and D. P. Stevenson, *J. Chem. Phys.*, **28**, 929 (1958).
(22) T. C. Farrar and E. D. Becker, "Pulse and Fourier Transform NMR", Academic Press, New York, N.Y., 1971, Chapter 2.
(23) (a) D. L. Vander Hart, H. S. Gutowsky, and T. C. Farrar, *J. Am. Chem. Soc.*, **89**, 5056 (1967); (b) T. C. Farrar and T. Tsang, *J. Res. Natl. Bur. Stand., Sect. A*, **73**, 195 (1969).
(24) (a) A. Carrington and A. D. McLachlan, "Introduction to Magnetic Resonance", Harper and Row, New York, N.Y., 1967, Chapter 5; (b) B. R. Appleman and B. P. Dailey, *Adv. Magn. Reson.*, **7**, 231 (1974).
(25) (a) E. R. Bernstein, W. C. Hamilton, T. A. Keiderling, S. J. La Placa, S. J. Lippard, and J. J. Mayerle, *Inorg. Chem.*, 11, 3009 (1972). (b) This is especially true in the case of the solid state x-ray diffraction results for $Zr(BH_4)_4$,[13a] and is probably responsible for some of the discrepancy between calculated and observed rigid lattice second moments.
(26) (a) H. Pfeifer, *NMR*, 7, 53 (1972); (b) G. Soda and H. Chihara, *J. Phys. Soc. Jpn.*, **36**, 954 (1974).
(27) (a) A. Kumar and C. S. Johnson, Jr., *J. Chem. Phys.*, **60**, 137 (1974). The nonexponentiality is most visible near the minimum and on the high-temperature side of ln T_1 vs. $1/T$ plots. (b) D. E. O'Reilly, E. M. Peterson, and T. Tsang, *Phys. Rev.*, **160**, 333 (1967). (c) M. Mehring and H. Raber, *J. Chem. Phys.*, **59**, 1116 (1973).
(28) P. Delise, G. Allegra, E. R. Mognaschi, and A. Chierico, *J. Chem. Soc., Faraday Trans. 2*, 71, 207 (1975).
(29) One possible solution to this time scale problem would be $T_{1\rho}$ measurements.[31a]
(30) (a) G. W. Smith, *J. Chem. Phys.*, **42**, 4229 (1965); (b) G. R. Miller and H. S. Gutowsky, *ibid.*, **39**, 1983 (1963).
(31) (a) S. Albert, H. S. Gutowsky, and J. A. Ripmeester, *J. Chem. Phys.*, **64**, 3277 (1976); (b) G. W. Smith, *ibid.*, **36**, 3081 (1962); (c) D. W. McCall and D. C. Douglas, *ibid.*, **33**, 777 (1960); (d) J. Kroon, *Philips Res. Rep.*, **15**, 501 (1960).
(32) S. E. Anderson, *J. Organomet. Chem.*, 71, 263 (1974).
(33) G. Binsch in ref 5a, Chapter 3.
(34) R. A. Schunn, C. J. Fritchie, Jr , and C. T. Prewitt, *Inorg. Chem.*, **5**, 892 (1966), and references cited therein.
(35) (a) The filled tridentate BH_4^- molecular orbitals[7a] consist, under C_{3v} symmetry, of a low-lying a_1 orbital and degenerate a_1 and e orbitals. The π molecular orbitals of C_3H_3 also consist of a lower energy a_1 orbital and an e set.[35b] (b) F. A. Cotton, "Chemical Applications of Group Theory", 2nd ed, Wiley, New York, N.Y., 1971, Chapter 7.
(36) T. Tsang and T. C. Farrar, *J. Chem. Phys.*, **50**, 3498 (1969).
(37) G. Arfken, "Mathematical Methods for Physicists", 2nd ed, Academic Press, New York, N.Y., 1973, Chapter 12.8.
(38) Computer program JMNMRS in FORTRAN IV for the CDC 6600.
(39) A. Watton, H. E. Petch, and M. M. Pintar, *Can. J. Phys.*, **48**, 1081 (1970).
(40) E. R. Andrew and G. E. Eades, *Proc. R. Soc. London, Ser. A*, **216**, 398 (1953).